Proceedings World Geothermal Congress 2023
Beijing, China, April 17 – 21, 2023

Harnessing Anthropogenic Heat from Radioactive Waste in Geological Disposal Facility settings via Closed-Loop Geothermal Systems

H.Doran, T.Renaud, I.Kolo, C.S.Brown, G. Falcone and D. Sanderson

James Watt School of Engineering, University of Glasgow, Glasgow, UK

h.doran.1@research.gla.ac.uk

Keywords: geological disposal facility (GDF), mined repository (MR), closed-loop geothermal system (CLGS), high-heat producing waste (HHPW).

ABSTRACT

Closed-loop geothermal systems (CLGS's) are useful concepts for heat extraction from the subsurface of low permeability. This paper addresses the possibility of a CLGS to recover waste heat and improve overall safety from a geological disposal facility (GDF). A 1 km lateral 'Eavor-like' U-tube closed-loop geothermal system (CLGS) was modelled within the T2Well-ECO2N/TOUGH2 software suite, to assess its long-term integrity and sustainability within a potential GDF environment. A preliminary 10-year numerical thermal analysis was investigated and compared against a model previously developed in MATLAB and OpenGeoSys (OGS) software, for three distinct geological environments suited for a GDF; evaporite (EV), higher strength (HSR) and lower strength sedimentary rock (LSSR). A static scenario (inactive wellbore) was also set up, where the heat profile emitted from canisters representative of high-heat producing waste (HHPW) was analysed over the same 10-year period. The results for the dynamic setup revealed a 0.1 °C temperature difference for T2Well-ECO2N/TOUGH2 against MATLAB/OGS with temperatures at the end of the lateral section to be 10.13 °C (EV), 8.46 °C (HSR) and 7.38 °C (LSSR) after 10-years. The static setup suggests the LSSR environment could benefit from the addition of the 'Eavor-like' U-tube CLGS to remove excess heat from the rock and improve overall GDF safety as temperatures exceed the bentonite buffer limitations (> 125 °C), while the EV and HSR environments fall within the acceptable criteria of < 100 °C. Overall temperature rises seen from the source at $\Delta T = 85$ °C (LSSR), $\Delta T = 54$ °C (HSR) and $\Delta T = 34$ °C (EV) after 10-years.

1. INTRODUCTION

Closed-loop geothermal systems (CLGS) are considered favourable to conventional geothermal methods for subsurface heat extraction within a low-permeability conductive rock setting. In addition, a geological disposal facility (GDF) that hosts radioactive waste also caters to a low permeable environment, to minimize pathways for possible radionuclide leakage into the surrounding formation. The safety of a GDF is paramount when devising a long-term solution to the disposal of radioactive waste and is one of the main reasons why GDF development has been continually delayed. From the UK's perspective, the construction phase cannot be implemented until a suitable geological site is chosen and approved – a recent national screening identified three regions of potential interest: two in Cumbria (Copeland and Allerdale) and one in Lincolnshire (Theddlethorpe) (RWM, 2021a, 2021b, 2021c; Waters et al., 2018). Even if 'perfect' geological conditions are present, long-term heat release (decay heat) from waste canisters can disrupt the local environment and could trigger additional thermal-hydro-mechanical-chemical (THMC) processes (Bernier et al., 2017).

This paper aims to combine both sectors by considering radioactive waste as an anthropogenic heat source term, where heat extraction from the subsurface is achieved using a 1 km 'Eavor-like' U-tube CLGS design. The design was modelled in T2Well-ECO2N/TOUGH2 and compared against a code developed in MATLAB (see Brown et al., 2022, 2021) and the OpenGeoSys (OGS) software (Chen et al., 2019) to provide a benchmark to assess its long-term integrity and sustainability in a GDF rock environment. This was followed by a static setup (inactive wellbore) to assess the temperature profile of conductive heat transfer emitted from 30 High-Heat Producing Waste (HHPW) canisters. The results presented are a continuation on previous work from Doran et al. (2022b) which adopted a semi-analytical/numerical modelling approach in identical GDF rock settings, with a focus on the addition of the heat source term within the geological environment. While the intended focus of this paper is on heat transfer within a conductive homogenous rock setting, understanding the temporal effects of the decay heat released from a GDF environment is crucial for future heterogeneity studies to improve the overall safety of the GDF. It could also provide a useful temperature profile on how much heat is available for recovery purposes and what proportion of this heat is safe to remove using the 'Eavor-like' U-tube CLGS design.

An outline on the GDF and CLGS settings is provided in Sections 2.1 and 2.2 respectively. A literature review on these technologies was previously presented in Doran et al. (2022b) and will therefore not be repeated within the contents of this paper. Section 2.3 introduces the concept of decay heat as an anthropogenic heat source within the GDF environment. A decay heat profile representative of an average high-heat producing waste canister (HHPW) from the UK inventory was adopted within this analysis for a 10-year disposal period, taken from Jackson et al. and RWM (2016; 2021d) – see Section 3.3. The methodology for the numerical setup is provided in Section 3.1.

2. BACKGROUND THEORY

2.1 GDF settings

A GDF can conform to different vertical depths between 0.2 – 5 km, as previously reported in Doran et al. (2022b). The lower end (0.2 – 1 km) is representative of a mined repository (MR), the conventional global route to long-term disposal of HHPW's (WNA, 2020). This concept tends to form a configuration of panels that extend laterally within the subsurface over many km's (Ikonen, 2007; Posiva Oy, 2012; Sundberg et al., 2009; Zhou et al., 2021a, 2021b). Existing underground rock laboratories aid the development of safe waste disposal into future MR's, such as those under construction in Sweden and Finland (Blechschmidt and Vomvoris, 2010; Posiva Oy, 2012; SKB, 2011). For the purposes of this paper, the GDF definition will apply to MR concepts (0.2 – 1 km), following

the UK's intended plan for HHPW disposal via the Swedish KBS-3V concept (SKB, 2013). 1 km was chosen as the maximum intended CLGS depth within an MR environment. Typical dimensions for one panel configuration of HHPW will depend on canister (p_x) and tunnel (p_y) spacing requirements – see Figure 1.

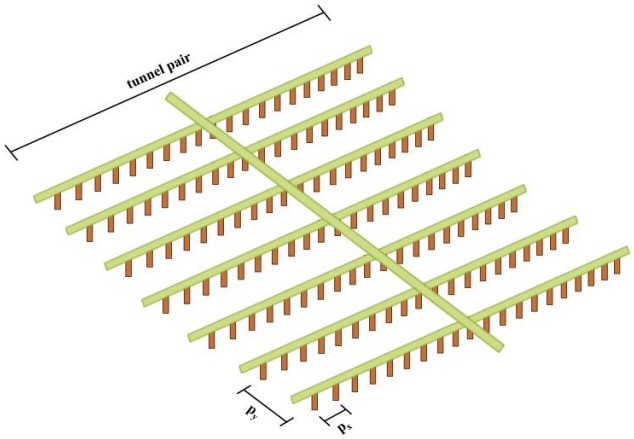

Figure 1: Schematic of a tunnel pair for a MR concept with canister (p_x) and tunnel (p_y) spacing dimensions defined, interpreted from (Ikonen, 2003, p.3).

According to Zhou et al (2021a), p_x and p_y vary between 6-10 m and 20-60 m, respectively. For the KBS-3V disposal concept, 50 canisters occupy 1 panel pair and so for a full panel with 30 access tunnels there is in total $50 \times 30 = 1500$ canisters present in one panel unit (Ikonen, 2003, p.3). With 50 canisters per tunnel, this provides a dimension range between 300-500 m across 1 tunnel (50 multiplied by p_x) and 600-1800 m across the 30 tunnels (30 multiplied by p_y). Another case study revealed a total length between access tunnels to be 1160 m ($p_y = 40$ m with 29 tunnels) (Sundberg et al., 2009). For the purposes of this paper, the lateral part of the 'Eavor-Like' U-tube CLGS is positioned along the p_y to consider one canister strip across the tunnels and omitting adjacent canisters in the p_x plane to enable a larger distance is covered for enhanced heat extraction. Other useful dimensions are for the canister itself that is encased in a copper shell with a height and outer diameter of approximately 5 m and 1 m respectively (Ikonen, 2007; Ikonen et al., 2018; Sundberg et al., 2009). Assuming a cylindrical canister, this suggests the heat source term should occupy an approximate volume of 3.9 m^3 – see Section 3.3 for source term setup. Further studies should investigate the addition of a bentonite buffer layer which is considered within the KBS-3V concept, where much of the decay heat is absorbed before it reaches the rock.

2.2 CLGS lateral settings

The lateral part of the 'Eavor-like' U-tube CLGS was modelled to reduce computational demand and to study the conductive heat transfer that will enter the lateral section from a GDF. A lateral length of 1 km was chosen as a lower limit to what is reported from the literature; previous studies have modelled lateral lengths between 1 - 2 km (Beckers et al., 2022) which can be defined as a sub divided region to suit MR dimensions reported from Section 2.1 (Sundberg et al., 2009; Tahir, 2022). It is important to make full use of the lateral footprint such that the decay heat released from each canister is captured to minimize heat release into the surrounding rock. Figure 2 below introduces the 1 km lateral CLGS concept within a GDF setting where canisters are situated below the wellbore, with T_{in} (inlet temperature), P_{in} (inlet pressure), L_l (lateral length) and $T_{e,l}$ (lateral end temperature):

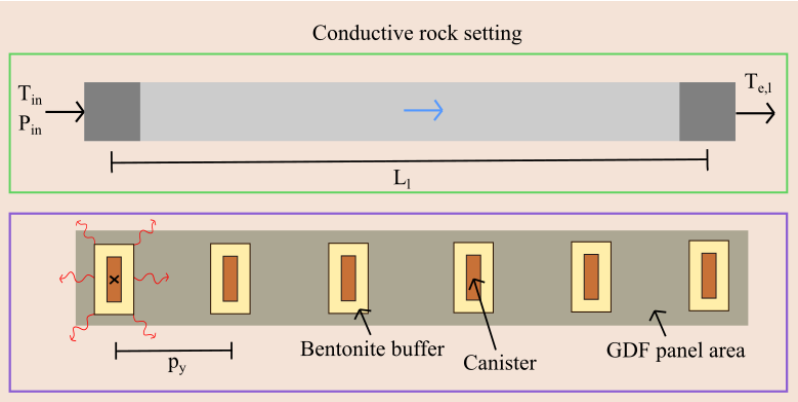

Figure 2: Schematic of 1 km lateral CLGS design within a GDF environment where canisters are separated by a distance p_y across tunnels. The dynamic wellbore study (see 3.2) and static heat source term study (3.3) are highlighted in green and purple textboxes respectively, where future work will combine the two. Note canister quantity is not to scale and the canister spacing p_x in Figure 1 has been omitted from this study to consider one strip of canisters only within the tunnel pair.

2.3 Decay heat as anthropogenic heat source term

Radioactive waste is a harmful by-product created from the generation of nuclear power that takes many forms, such as spent-nuclear fuel (SNF) or high-level waste (HLW) that has undergone additional reprocessing activities. For each type of waste, a mixture of radionuclides exists within the waste form that continually evolve with time. This unique blend ultimately defines the total activity residing within the fuel and hence the quantity of decay heat released at a specific point in time. This paper discusses the concept of recovering this decay heat from a generic HHPW canister that is intended for GDF disposal.

The decay heat emitted from a waste form is calculated via equation (1) below:

$$D_T = \sum_{i=1}^{M} A_i^T(t)\left[E_{i,HP}^t + E_{i,LP}^t + E_{i,EM}^t\right] = \sum_{i=1}^{M} A_i^T(t)E_T^i = A_T \times E_T \tag{1}$$

where A_T is the total activity at time t and E_T is the total energy released per decay from all i radionuclides. The latter term is a summation of decay interactions arising from heavy particles (alpha, mean-recoil), light particles (beta, auger-electrons, conversion electrons) and electromagnetic energy (gamma, x-ray, internal bremsstrahlung) (Nichols, 2015, 2002). The accuracy of this decay heat is primarily dependent on nuclear data taken from evaluated libraries that feed the radionuclide inventory. A recent study revealed that discrepancies in six fission products across six evaluated nuclear libraries could alter the true decay heat vs cooling time relationship when considering generic Magnox fuel for a pre-irradiation of 5.3 years and post-irradiation timescales between 1 – 100 ky (Doran et al., 2022a).

Prior to disposal, the temporal evolution of the decay heat will depend on pre-irradiated conditions inside the reactor (nuclear fission, neutron capture and radioactive decay processes) and post-irradiated conditions during the back-end stages of the fuel cycle such as conditioning, reprocessing, and the interim storage period (natural radioactive decay). As such, it is important to quantify the initial decay heat at the time of repository deposition (pre-cooling period). Across the literature, 1 – 2 kW/t of initial decay heat prior to disposal is presumed for a typical HHPW canister (Ikonen, 2007; Ikonen et al., 2018; Sundberg et al., 2009; Zhou et al., 2021a). However, this often assumes an open-loop fuel cycle where the waste type spends up to 50 years in interim storage. On the contrary, the UK's HHPW waste inventory could involve a pre-cooling period greater than 50 years, especially for reprocessed waste following a closed-loop cycle and accounting for additional interim storage time while awaiting a permanent GDF site.

The decay heat vs cooling time relationship during long-term disposal (post-irradiation) can be simplified by an exponential decay function, defined in equation (2) below:

$$D(t) = D(0)\sum_{i=1}^{j} a_i e^{-t/t_i} \tag{2}$$

where $D(0) = D_T$ is the initial heat output prior to disposal at time T, t is the time spent during disposal (post-irradiation), and a_i/t_i are constant coefficients/time coefficients for a set of post-irradiated times $i = j$. Within this paper, a HHPW canister reported in Jackson et al.(2016) was used as the anthropogenic heat source term with initial decay heat 2117.4 W at disposal deposition – see Section 3.3. However, care should be taken with this estimation and future work will involve assessing all UK HHPW types to understand their evolution throughout the interim storage period, to gain an accurate depiction of $D(0)$ prior to disposal.

3. METHODOLOGY

3.1 T2Well-ECO2N/TOUGH2 software setup

T2Well-ECO2N/TOUGH2 is a coupled wellbore/reservoir simulator intended for multi-phase non-isothermal flow (Pan and Oldenburg, 2014). The equation of state (ECO2N) is conventional to non-isothermal water – salt – carbon dioxide fluid mixtures under temperature and pressure constraints of $10\ ℃ < T < 300\ ℃$ and $P < 600$ bar (Pan et al., 2015). Pure water has been adopted within this paper to continue from the work previously accomplished in Doran et al. (2022b), and therefore all salt and carbon dioxide mass fractions were set to zero. The conservation equations were solved numerically using the integral finite volume method in a 3D radial to cartesian mesh structure (see 3.2), albeit the wellbore which adopts a 1D Drift Flux Model to solve the single-phase momentum equation (Pan *et al*., 2011) – see Table 1 below interpreted from (Pan et al., 2011; Pan and Oldenburg, 2014).

From Table 1, the general conservations equations for the reservoir (3) and wellbore (8) consist of mass accumulation (M^m), mass flux (F^m), energy accumulation (M^E) and energy flux (F^E) terms. Note that equations (4) and (5) for the reservoir are set to zero due to conductive rock settings (zero porosity and no liquid velocity present within rock pores). Equation (13) is representative of the momentum equation where the drift flux velocity is equal to zero under single-phase flow (Pan et al., 2011, p.50). The other terms within Table 1 are: q^κ source/sink terms, ρ_R rock density, c_R rock specific heat capacity, X_L mass fraction of liquid phase, ρ_L liquid density, S_L local saturation of liquid phase, U_L internal energy of liquid phase, u_L liquid velocity of fluid, g gravitational acceleration, z elevation in well, θ inclination angle of wellbore, k area averaged thermal conductivity of wellbore, σ cross section area of wellbore, h_L specific enthalpy of liquid phase, γ slip between two phases, f apparent friction coefficient, Γ surface area of well side and P pressure.

Other TOUGH codes have been previously applied to repository settings; for example, to assess thermal-hydraulic behaviour of Callo-Oxfordian Clay following gas and decay heat release in France using TOUGH-MP (Poller et al., 2011), to model radionuclide transport for the Forsmark and Gorleben sites in Sweden and Germany, respectively, using TOUGHREACT (Schwartz, 2012a, 2012b) and to model THMC processes in buffer material at the Mont Terri and Grimsel underground rock laboratories in Switzerland (Lee et al., 2021) using TOUGH2-MP/FLAC3D. For this study a coupled wellbore-reservoir simulator is needed (T2Well/TOUGH2) to model the subsurface and the 'Eavor-like' U-tube design. T2Well-EOS1 has been recently modelled for a Deep Borehole Heat

Exchanger (DBHE) within an enhanced conductive setting (Doran et al., 2021; Renaud et al., 2021). In addition, T2Well-ECO2N has been applied to a U-tube CLGS system (1.1 km lateral section) for CO_2 and pure water fluids in Oldenburg et al. (2019). This combined a semi-analytical/numerical hybrid for the vertical/lateral sections of the CLGS respectively to reduce computational costs. For the purposes of this paper, a pure numerical model has been produced in T2Well-ECO2N/TOUGH2 but for the CLGS lateral section only – see Section 3.2 below.

Table 1. Key conservation equations for the reservoir (TOUGH2) and wellbore (T2Well-ECO2N) under single phase flow, interpreted from Pan et al (2014).

Reservoir Conservation Equations	Wellbore Conservation Equations
$\frac{d}{dt}\int_{V_n} M^\kappa \, dV_n = \int_{\Gamma_n} F^\kappa \cdot n d\Gamma_n + \int_{V_n} q^\kappa \, dV_n$ (3)	$\frac{\partial M^\kappa}{\partial t} = q^\kappa + F^\kappa$ (8)
$M^m = 0$ (4)	$M^m = \rho_L S_L X_L^\kappa$ (9)
$F^m = 0$ (5)	$F^m = -\frac{1}{\sigma}\left[\frac{d(\sigma \rho_L S_L X_L^\kappa u_L)}{dz}\right]$ (10)
$M^E = \rho_R c_R T$ (6)	$M^E = \rho_L S_L \left(U_L + \frac{u_L^2}{2} + gz\cos\theta\right)$ (11)
$F^E = -k\frac{\partial T}{\partial z}$ (7)	$F^E = -k\frac{\partial T}{\partial z} - \frac{1}{\sigma}\frac{\partial}{\partial z}\left[\sigma \rho_L S_L u_L \left(h_L + \frac{u_L^2}{2} + gz\cos\theta\right)\right]$ (12)
	$\frac{\partial}{\partial t}(\rho_L u_L) + \frac{1}{\sigma}\frac{\partial}{\partial z}[\sigma(\rho_L u_L^2 + \gamma)] = -\frac{\partial P}{\partial z} - \frac{\Gamma f \rho_L \lvert u_L \rvert u_L}{2\sigma} - \rho_L g\cos\theta$ (13)

3.2 1 km 'Eavor-like' U-tube CLGS preliminary setup

A radial to cartesian mesh structure was created using a python script incorporating the pygmsh and toughio libraries to pre-process into T2Well-ECO2N/TOUGH2 (Luu, 2020; Schlömer, 2021). This transitional grid was created to ensure the anthropogenic heat source terms are located below the 1 km lateral section of the U-tube, within the cartesian part of the grid, whilst maintaining a radial structure close to the wellbore. In addition, this mesh follows a similar transitional grid to that achieved in the literature for T2Well-ECO2N for the CLGS in Oldenburg et al. (2019). Constant temperature (Dirichlet) and no-flux (Neumann) were set to all outer boundaries of the model. Figure 3 displays the dimensional structure of the mesh with a close-up depiction of the wellbore (in red):

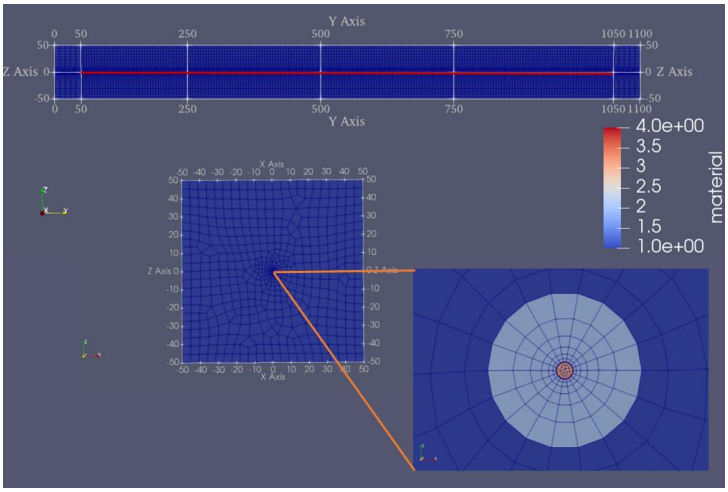

Figure 3: 3D radial to cartesian mesh constructed for T2Well-ECO2N/TOUGH2. Dimensions are 50 m × 50 m × 1100 m in the x, z, y axes, respectively. The wellbore was extruded in the y-domain from 50 m to 1050 m and with max grid size 5 m.

Table 2 below illustrates the parameters adopted within the long-term sustainability assessment, alongside rock thermal properties, taken from a previous CLGS case study (Yuan et al., 2021). The parameters adopted in Table 2 were also applied in the finite-difference model developed previously in MATLAB (see Brown et al., 2022, 2021) and finite element OGS numerical software (Chen et al., 2019; Watanabe et al., 2017) - their governing equations are reported elsewhere for reference. A 3D cartesian mesh was created where heat flux in the subsurface was solved using the dual-continuum method, assuming constant fluid properties for pure water. This involves treating the wellbore as a 1D line in a 3D medium which represents the surrounding rock. On the contrary, T2Well-ECO2N/TOUGH2 utilises the drift-flux model and non-constant water properties dependent on the specified equation of state ECO2N.

Table 2: 'Eavor-like' U-tube CLGS 1 km lateral design parameters (left) and GDF rock thermophysical properties (right)

Long-term sustainability setup[1]	GDF thermophysical rock properties[2]
Geometry lateral: $R_i = 0.105\ m$, $R_o = 0.115\ m$, $L_l = 1\ km$	***EV:*** $k_{EV} = 4.8\ W/mK$, $c_{P,EV} = 860\ J/kgK$, $\rho_{EV} = 2500\ kg/m^3$
Reservoir conditions: $T_{i,R} = 31℃$, $P_{i,R} = 10\ MPa$	***HSR:*** $k_{HSR} = 3.0\ W/mK$, $c_{P,HSR} = 820\ J/kgK$, $\rho_{HSR} = 2700\ kg/m^3$
Wellbore fluid conditions: $\dot{m} = 5.47\ kg/s$, $T_{in} = 5\ ℃$	***LSSR:*** $k_{LSSR} = 1.9\ W/mK$, $c_{P,LSSR} = 1400\ J/kgK$, $\rho_{LSSR} = 2100\ kg/m^3$
[1] Wellbore Inner/outer radii R_i/R_o, initial temperature/pressure at 1 km depth $T_{i,R}/P_{i,R}$, mass flow rate $\dot{m}$ and inlet temperature T_{in} . [2] Thermal conductivity k, specific heat capacity c_P and density ρ of rock.	

3.3 Anthropogenic heat source term setup

The same mesh structure as in Section 3.2 was adopted for the investigation of a static case where the wellbore is inactive (no fluid flow) and assumed to have the same properties as those of the GDF formation illustrated in Table 2. This was to investigate how the decay heat released from canisters from the GDF environment may alter the temperature profile within the rock over a 10-year period, as decay heat from nuclear waste canisters may disturb the thermo-hydromechanical state of the repository. Heat distribution from a source term due to conduction/diffusion will depend on a diffusion distance d_{diff}(m), see equation (14) below (Jackson et al., 2016, p.14):

$$d_{diff}(m) = \sqrt{2t\frac{k_R}{c_{P,R}\rho_R}} = \sqrt{2\alpha t} \tag{14}$$

where α is the thermal diffusivity of the rock (subscript R). This means that 10 years after GDF waste emplacement, heat will spread a distance of $d_{diff} = 37.5, 29.2$ and 20.2 m away from the canister for host rock environments EV, HSR and LSSR, respectively, unless the heat is artificially removed. According to Hökmark et al. (2009, pp 25-26), heat flux is assumed to spread radially out from the centre of the canister into the surrounding rock and is dominated by a temperature gradient ΔT characteristic of the thermal properties of each material the heat is distributed through. For this study, only the thermal properties of the rock are presumed, as the focus is heat dispersion within the GDF environment. However, a future detailed study on the thermal properties of each layer (canister, bentonite buffer etc) is needed to accurately determine the temperature gradient from the centre.

Assuming a canister volume of 3.9 m^3 (see Section 2.1), 5 cells (1 centre cell surrounded by 4 nearest neighbours) were picked to represent the anthropogenic heat source term yielding a total volume of $\approx$ 3.7 m^3 – see the pink cells in Figure 4b. A python script was developed to input each $D(t)$(W) value to act as a time-step function for the exponential decay heat relationship, due to constant heat flux generation limitations in TOUGH2 to account for temporal heat source terms. Each simulation produced 10 output files, with $D(t = 0)$ = 2117.40 W, $D(t = 1)$ = 2023.93 W, $D(t = 2)$ = 1957.73 W, … $D(t = 10)$ = 1670.58 W to illustrate the change in decay heat (Figure 2a) at each yearly interval. In addition, the decay heat was equally split between the 5 cells such that $D(t = 0)$ = 2117.40/5 = 423.48 W In total, 30-point sources were inserted into the model from y = 57.5 m to y = 927.5 m, spaced $p_y = 30$ m apart to represent a strip of canisters across adjacent tunnels of a MR panel (see 2.1). The temperature profile from 1 – 10 years was recorded as a 2D slice for each GDF environment (EV, HSR and LSSR) – see Section 4.2.

a)

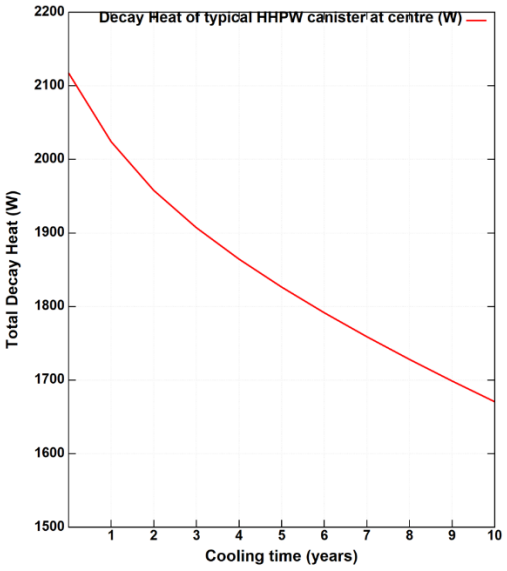

b)

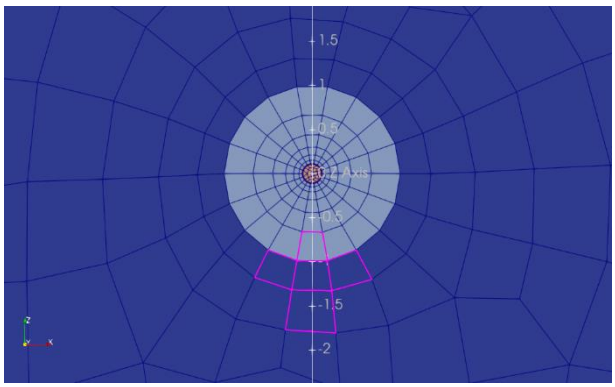

Figure 4: a) Decay heat vs cooling time profile at canister centre (red) 10 years after waste emplacement sourced from Jackson et al. (2016), b) Heat source term (pink cells) equating to a total volume of $\approx$ 3.7 m^3 approximately 1 m away from wellbore.

4. RESULTS

Section 4.1 depicts the benchmarking results to assess long-term sustainability of the 1 km lateral design with a constant circulation flow rate for 10 years, and Section 4.2 illustrates the temperature profile for the heat source term emitted from a HHPW canister near the start of wellbore injection point fixed at y = 57.5 m (see Section 3.3) with no fluid flow through the wellbore:

4.1 Long-term sustainability comparison of 1 km lateral 'Eavor-like' U-tube CLGS

Figure 5 below depicts a 10-year long-term sustainability assessment (outlet) temperature profile recorded at the end of the 1 km lateral 'Eavor-like' U-tube CLGS installation in T2Well-ECO2N/TOUGH2 (red) against the MATLAB (blue) and OGS (green) numerical codes, within the three GDF rock environments EV (solid line), HSR (dashed line) and LSSR (dot dashed line):

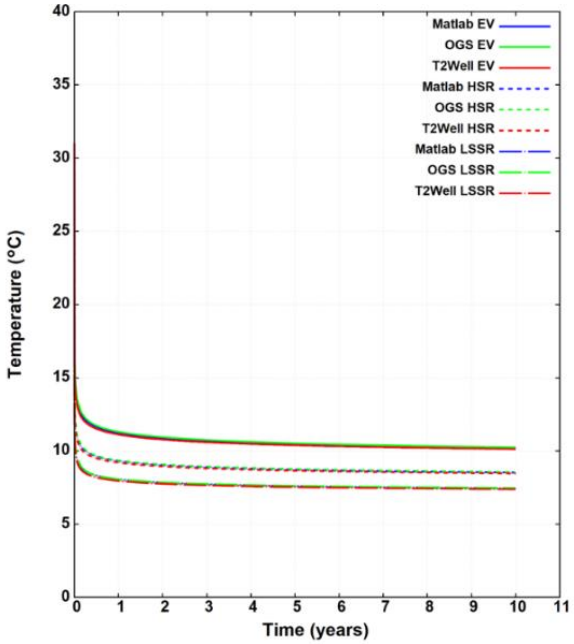

Figure 5: Temperature vs time long-term sustainability assessment on 1 km lateral 'Eavor-like' U-tube CLGS, against MATLAB and OGS software within the GDF environments: EV (solid), HSR (dashed) and LSSR (dot dashed).

From Figure 5, the temperatures estimated at the end of the 1 km lateral 'Eavor-like' U-tube CLGS design at 10 years for T2Well-ECO2N/TOUGH2 was 10.13 °C, 8.46 °C and 7.38 °C for the EV, HSR and LSSR rock environments, respectively. In general, MATLAB and OGS produced near identical results for all cases, which accounts for OGS data overlying the data produced from MATLAB, as also identified in previous studies (Doran et al., 2022b). This is because both models adopt the dual continuum method (and thermal resistances models) to approximate heat transfer between the lateral section of the wellbore and the surrounding rock. However, there is a slight underestimation in temperature by T2Well-ECO2N/TOUGH against the other software of approximately 0.1 °C, revealing percentage differences for each rock environment of: EV - 1.15 % (OGS) and 1.06 % (MATLAB), HSR - 1.23 % (OGS) and 0.92 % (MATLAB), LSSR - 1.15 % (OGS) and 0.85 % (MATLAB) at 10 years. This could be due to the methods adopted to compute fluid flow within the design; for example, T2Well-ECO2N adopts the drift-flux model, while MATLAB and OGS use the dual-continuum method. It is unlikely for this scenario that the differences are due to non-constant fluid properties previously highlighted in (Doran et al., 2022b) because vertical depth and geothermal gradient were not considered, which will affect the fluid properties more prominently. As a constant mass flow rate was applied, this leads to rapid cooling of the CLGS (see Figure 5) within the first year of operation. Future work on the long-term sustainability temperature profile is needed to assess how this rapid cooling effect is influenced by the addition of heat from a GDF and whether an additional heat pump system is needed to utilise the recovered heat.

4.2 Static 10-year temperature profile in EV, HSR and LSSR environments

Figure 6 illustrates a 2D temperature profile slice in the xz plane (fixed y = 57.5 m) – see Figures 3 and 4b - where the first source term was emplaced, for the EV, HSR and LSSR environments respectively:

The maximum temperatures seen at the centre of the source (canister) were 71.97 °C and 65.27 °C (EV), 95.33 °C and 85.37 °C (HSR), and 128.59 °C and 115.68 °C (LSSR) for t = 1 and t = 10 years respectively. When the source term decayed from 2117.4 W to 1670.58 W across this 10-year period the temperature gradients seen at the centre of the source term were $\Delta T = 6.7$ ℃ (EV), $\Delta T = 9.96$ ℃ (HSR) and $\Delta T = 12.91$ ℃ (LSSR). In addition, the HSR 1 year case approximately matches to literature reported in Ikonen (2003) where a line source of similar decay heat and rock settings reached 80 °C after 2 years. With 31 °C as the initial rock temperature – see Table 2 – the temperature spread is seen to extend far out into the rock domain with an observed rock temperature increase after 10-years of approximately 5 °C (EV) 7 m away, 5 °C (HSR) 7 m away and 5 °C (LSSR) 10 m radially away from the source term. This radial distance < 10 m lies within the bentonite buffer layer and excavated deformation zone (EDZ) and so temperature gradients here are critical to assess long term integrity of the GDF (Sasaki and Rutqvist, 2022; Siren et al., 2015). In addition, the 2D temperature profiles seen in Figure 6 are nearly identical to all 30 canisters, with minor differences in temperature seen between the outer and central canister, concluding there is minimal thermal interference after 10 years. The results conclude that the LSSR rock environment exhibits the slowest conductive heat transfer away from the point source as a higher ΔT is seen at the

source in comparison to the EV environment under the same decay heat vs cooling time relationship (factor of 2.5 higher). The radial thermal spread is also slower with more cells exhibiting the same initial temperature of 31 °C after 10 years. This is due to LSSR's lower thermal diffusivity in comparison to the EV rock of highest thermal diffusivity. The LSSR rock environment also shows a temperature increase of approximately 50 °C at the source after 10-years in comparison to the EV case. Indeed, it was shown in Zhou et al. (2021a) that decreasing the rock's thermal conductivity increases the peak temperatures seen at the buffer interface, proving the importance of this parameter on overall thermal heat transfer.

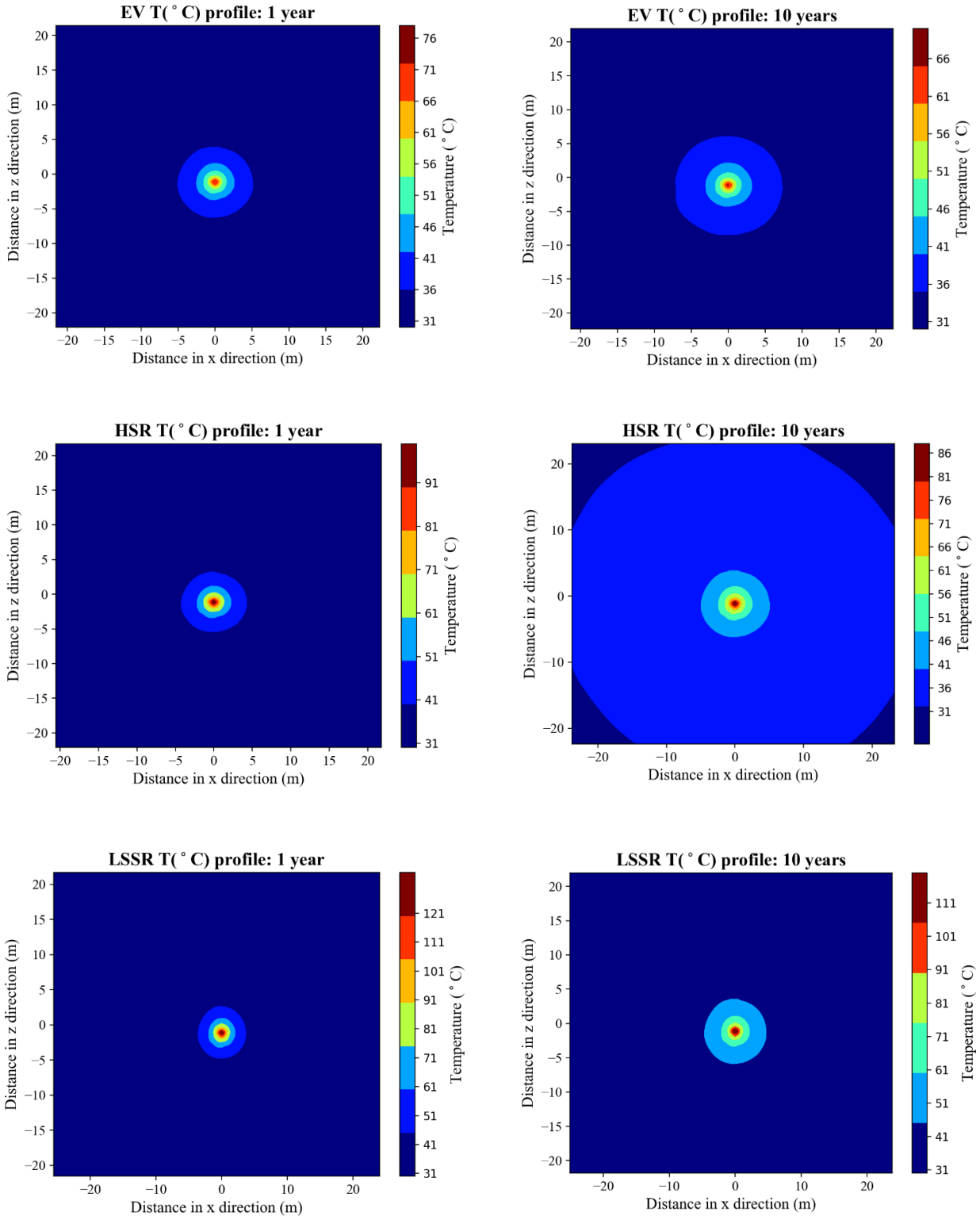

Figure 6: Temperature in xz plane (y = 57.5 m) where source term is situated approximately 1 m away from the wellbore. Left and right images illustrate the change in temperature profile after 1 year and 10-years. Colour map illustrates associated temperature gradient in each environment; EV (6a,6b), HSR (6c,6d) and LSSR (6e,6f). Figures zoomed in to see ΔT contours.

From a GDF safety perspective, the temperature at the bentonite buffer interface should not exceed 100 °C to minimize canister corrosion (Hedin, 1999; SKB, 2011). Therefore, the EV and HSR environments are seen to match this criterion across the 10-year

period and is most feasible from a GDF safety perspective. However, there are ongoing studies for temperatures > 100 °C – for example the HE-E experiment at the Mont Terri site in Switzerland is looking at 140 °C in Opalinus Clay (Gens et al., 2020). In addition, a maximum buffer limit can be stretched to 125°C for the Opalinus clay environment (LSSR) (NAGRA, 2002, p.109). This means the temperatures from the 1-year LSSR case exceeds this limit but is feasible after 10 years so could pose additional safety concerns with THMC processes. One way to overcome these safety concerns is to implement the 'Eavor-like' U-tube CLGS into the LSSR environment, such that excess heat is drawn into the design, and thus reduce the rock temperature to a suitable value to conform to the buffer safety limits. Depending on the overall thermal spread and how much 'additional' heat has been dispersed into the rock, the LSSR environment could provide the highest heat extraction into the 1 km 'Eavor-like' U-tube CLGS design, especially with the largest $\Delta T = 101$ °C compared to $\Delta T = 83$ °C (HSR) and $\Delta T = 41$ °C (EV) after 10-years from the centre of the source out to 2 m in the rock. A future study could investigate the ideal distance of the 1 km 'Eavor-like' U-tube CLGS design from the point source, such that the temperature gradient in the rock is reduced and maximal heat recovery is achieved.

Future work should also investigate the heat spread on a 3D plot to reveal the hidden temperature profile along the y-axes (across tunnels) and if there is any interference between each source term. In addition, a larger footprint of the MR could also be modelled to account for canisters either side of the central strip investigated within this study, and how increasing the number of canisters effects the extent of heat transfer in the surrounding rock. This study has also focused on homogenous rock– in reality, a heterogenous setting could be modelled for a future UK GDF site highlighted in section 1, and accounting for a measured depth profile to compare changes in the natural geothermal gradient after anthropogenic heat source term addition.

5. CONCLUSIONS

In conclusion, the 10-year long-term sustainability study for the 1 km 'Eavor-like' U-tube CLGS design yielded temperatures at the end of the lateral of 10.13 °C, 8.46 °C and 7.38 °C for the EV, HSR and LSSR rock environments respectively. A good comparison was also made against a code developed in MATLAB and the OGS software where only a 0.1 °C difference was seen between T2Well-ECO2N/TOUGH2 and MATLAB/OGS. The static anthropogenic heat source term setup revealed for 1 canister in the xz plane maximum canister temperatures at the centre cell to be EV: 71.97 °C and 65.27 °C, HSR: 95.33 °C and 85.37 °C, LSSR: 128.59 °C and 115.68 °C for 1 and 10 years respectively when the source term decayed from 2117.4 W to 1670.58 W. A change in the initial temperature environment > 31 °C was seen in all scenarios and after 10-years approximate rock temperature increases of 5 °C (EV) 7 m away, 5 °C (HSR) 7 m away and 5 °C (LSSR) 10 m away. The overall temperature rise from the initial rock gradient was $\Delta T = 85$ °C (LSSR), $\Delta T = 54$ °C (HSR) and $\Delta T = 34$ °C (EV) after 10-years. From a GDF safety perspective, the LSSR environment could benefit from the addition of an 'Eavor-like' U-tube CLGS to draw heat away from the rock and prevent temperatures exceeding buffer safety limits (> 125 °C), while the EV and HSR rock temperature fell within range of the buffer temperature criteria after 10 years. In addition, the LSSR rock yields the highest ΔT away from the source by a factor of 2.5 which could provide the highest heat extraction rate into the 1 km 'Eavor-like' U-tube CLGS design. Future work on a dynamic setup of the 1 km 'Eavor-like' U-tube CLGS design in the LSSR rock setting with the 'new' temperature profile is needed to determine the proportion of heat that will be removed from the rock into the wellbore and how this can mitigate THMC processes. This will be of particular importance for the LSSR environment to remove excess heat from the rock into the 'Eavor-like' U-tube CLGS to improve overall GDF safety.

ACKNOWLEDGEMENTS

The authors would like to acknowledge additional assistance from colleagues at Lawrence Berkeley National Laboratory, in particular: Dr Keurfon Luu who created the T2Well mesh using toughio and Dr Yingqi Zhang for assisting in compilation of the T2Well-ECO2N/TOUGH2 software.

FUNDING

This research is supported by the UK Engineering and Physical Sciences Research Council (EPSRC) [Grant number: EP/R513222/1].

REFERENCES

Beckers, K.F., Rangel-Jurado, N., Chandrasekar, H., Hawkins, A.J., Fulton, P.M., Tester, J.W., 2022. Techno-Economic Performance of Closed-Loop Geothermal Systems for Heat Production and Electricity Generation. Geothermics 100, 102318.

Bernier, F., Lemy, F., De Cannière, P., Detilleux, V., 2017. Implications of safety requirements for the treatment of THMC processes in geological disposal systems for radioactive waste. J. Rock Mech. Geotech. Eng. 9, 428–434.

Blechschmidt, I., Vomvoris, S., 2010. Underground research facilities and rock laboratories for the development of geological disposal concepts and repository systems. In: Ahn, J., Apted, M.J. (Eds.), Geological Repository Systems for Safe Disposal of Spent Nuclear Fuels and Radioactive Waste. Woodhead Publishing, pp. 82–118.

Brown, C.S., Cassidy, N.J., Egan, S.S., Griffiths, D., 2021. Numerical modelling of deep coaxial borehole heat exchangers in the Cheshire Basin, UK. Comput. Geosci. 152, 104752.

Brown, C.S., Cassidy, N.J., Egan, S.S., Griffiths, D., 2022. A sensitivity analysis of a single extraction well from deep geothermal aquifers in the Cheshire Basin, UK. Q. J. Eng. Geol. Hydrogeol. 1–17.

Chen, C., Shao, H., Naumov, D., Kong, Y., Tu, K., Kolditz, O., 2019. Numerical investigation on the performance, sustainability, and efficiency of the deep borehole heat exchanger system for building heating. Geotherm. Energy 7, 1–26.

Doran, H.R., Cresswell, A.J., Sanderson, D.C.W., Falcone, G., 2022a. Nuclear data evaluation for decay heat analysis of spent nuclear fuel over 1–100 k year timescale. Eur. Phys. J. Plus 2022 1376 137, 1–17.

Doran, H.R., Renaud, T., Brown, C.S., Kolo, I., Falcone, G., Sanderson, D.C.W., 2022b. Radioactive waste as an anthropogenic heat source: shallow and deep geothermal applications. In: Submitted to: European Geothermal Congress. Berlin, p. 7.

Doran, H.R., Renaud, T., Falcone, G., Pan, L., Verdin, P.G., 2021. Modelling an unconventional closed-loop deep borehole heat exchanger (DBHE): sensitivity analysis on the Newberry volcanic setting. Geotherm. Energy 9, 1–24.

Gens, A., De Vasconcelos, R.B., Olivella, S., 2020. Towards higher temperatures in nuclear waste repositories. E3S Web Conf. 205, 01001.

Hedin, A., 1999. Deep repository for spent nuclear fuel. SR 97 - Post-closure safety. Main Report. Stockholm.

Hökmark, H., Lönnqvist, M., Kristensson, O., Sundberg, J., Hellström, G., 2009. Strategy for thermal dimensioning of the final repository for spent nuclear fuel. Stockholm.

Ikonen, K., 2003. Thermal analyses of spent nuclear fuel repository. Helsinki.

Ikonen, K., 2007. Thermal Analysis of Repository for Spent EPR-type Fuel. Olkiluoto.

Ikonen, K., Kuutti, J., Raiko, H., 2018. Thermal Dimensioning for the Olkiluoto Repository - 2018 Update. Eurajoki.

Jackson, C.P., Holton, D., Myers, S., 2016. Project Ankhiale: Estimating the uplift due to high-heat-generating waste in a Geological Disposal Facility . Warrington.

Lee, C., Lee, J., Kim, G.Y., 2021. Numerical analysis of coupled hydro-mechanical and thermo-hydro-mechanical behaviour in buffer materials at a geological repository for nuclear waste: Simulation of EB experiment at Mont Terri URL and FEBEX at Grimsel test site using Barcelona basic model. Int. J. Rock Mech. Min. Sci. 139, 104663.

Luu, K., 2020. toughio: Pre- and post-processing Python library for TOUGH. J. Open Source Softw. 5, 1–3.

NAGRA, 2002. Project Opalinus Clay Safety Report Demonstration of disposal feasibility for spent fuel, vitrified high-level waste and long-lived intermediate-level waste. Wettingen.

Nichols, A.L., 2002. Nuclear Data Requirements for Decay Heat Calculations. Vienna.

Nichols, A.L., 2015. Recommended decay data and evaluated databases – international perspectives. J. Nucl. Sci. Technol. 52, 17–40.

Oldenburg, C., Pan, L., Muir, M., Oldenburg, C.M., Muir, M.P., Eastman, A.D., Higgins, B.S., 2019. Numerical Simulation of Critical Factors Controlling Heat Extraction from Geothermal Systems Using a Closed-Loop Heat Exchange Method. In: 41st Workshop on Geothermal Reservoir Engineering. Lawrence Berkeley National Laboratory, Stanford, pp. 1–8.

Pan, L., Oldenburg, C.M., 2014. T2Well—An integrated wellbore–reservoir simulator. Comput. Geosci. 65, 46–55.

Pan, L., Oldenburg, C.M., Wu, Y.-S., Pruess, K., 2011. T2Well/ECO2N Version 1.0: Multiphase and Non-Isothermal Model for Coupled Wellbore-Reservoir Flow of Carbon Dioxide and Variable Salinity Water. Berkeley.

Pan, L., Spycher, N., Doughty, C., Pruess, K., 2015. ECO2N V2.0: A TOUGH2 Fluid Property Module for Mixtures of Water, NaCl, and CO2. Berkeley.

Poller, A., Enssle, C.P., Mayer, G., Croisé, J., Wendling, J., 2011. Repository-Scale Modeling of the Long-Term Hydraulic Perturbation Induced by Gas and Heat Generation in a Geological Repository for High-and Intermediate-Level Radioactive Waste: Methodology and Example of Application. Transp. Porous Media 90, 77–94.

Posiva Oy, 2012. Olkiluoto Site Description 2011. Olkiluoto.

Renaud, T., Pan, L., Doran, H., Falcone, G., Verdin, P.G., 2021. Numerical Analysis of Enhanced Conductive Deep Borehole Heat Exchangers. Sustain. 13, 1–21.

RWM, 2021a. Search Area Evaluation Report: Allerdale Search Area and the adjacent inshore area. Didcot.

RWM, 2021b. Search Area Evaluation Report: Mid Copeland Search Area and the adjacent inshore area . Didcot.

RWM, 2021c. Initial Evaluation Report: Theddlethorpe Gas Terminal Site and surrounding area within the East Lindsey Area . Didcot.

RWM, 2021d. Inventory for geological disposal Main Report. Didcot.

Sasaki, T., Rutqvist, J., 2022. Effects of time-dependent deformation of shale on the integrity of a geological nuclear waste repository. Int. J. Rock Mech. Min. Sci. 158, 105206.

Schlömer, N., 2021. pygmsh: A Python frontend for Gmsh.

Schwartz, M.O., 2012a. Modelling radionuclide transport in large fractured-media systems: The example of Forsmark, Sweden. Hydrogeol. J. 20, 673–687.

Schwartz, M.O., 2012b. Modelling groundwater contamination above a nuclear waste repository at Gorleben, Germany. Hydrogeol. J. 20, 533–546.

Siren, T., Hakala, M., Valli, J., Kantia, P., Hudson, J.A., Johansson, E., 2015. In situ strength and failure mechanisms of migmatitic gneiss and pegmatitic granite at the nuclear waste disposal site in Olkiluoto, Western Finland. Int. J. Rock Mech. Min. Sci. 79, 135–148.

SKB, 2011. Long-term safety for the final repository for spent nuclear fuel at Forsmark Main report of the SR-Site project Volume I. Stockholm.

SKB, 2013. Design and production of the KBS-3 repository. Updated 2013-10. Stockholm.

Sundberg, J., Back, P.-E., Christiansson, R., Hökmark, H., Ländell, M., Wrafter, J., 2009. Modelling of thermal rock mass properties at the potential sites of a Swedish nuclear waste repository. Int. J. Rock Mech. Min. Sci. 46, 1042–1054.

Tahir, M.U., 2022. Radioactive waste management: Geological disposal facilities (GDF's) and deep boreholes disposal (DBD) opportunities for heat recovery. University of Glasgow.

Watanabe, N., Blöcher, G., Cacace, M., Held, S., Kohl, T., 2017. Theory. In: Geoenergy Modeling III - Enhanced Geothermal Systems, SpringerBriefs in Energy. Springer International Publishing, Cham, pp. 1–110.

Waters, C., Schofield, D., Evans, D.E., Millward, D., Haslam, R., Ó'Dochartaigh, B., Bloomfield, J.P., Lee, J.R., Baptie, B., Shaw, R.P., Bide, T., McEvoy, F.M., 2018. National Geological Screening: Northern England. CR/17/103.

WNA, 2020. Storage and Disposal Options for Radioactive Waste [WWW Document]. URL https://www.world-nuclear.org/information-library/nuclear-fuel-cycle/nuclear-waste/storage-and-disposal-of-radioactive-waste.aspx (accessed 4.24.20).

Yuan, W., Chen, Z., Grasby, S.E., Little, E., 2021. Closed-loop geothermal energy recovery from deep high enthalpy systems. Renew. Energy 177, 976–991.

Zhou, X., Sun, D., Xu, Y., 2021a. A new thermal analysis model with three heat conduction layers in the nuclear waste repository. Nucl. Eng. Des. 371, 110929.

Zhou, X., Xu, Yunshan, Sun, D., Tan, Y., Xu, Yongfu, 2021b. Three-dimensional thermal–hydraulic coupled analysis in the nuclear waste repository. Ann. Nucl. Energy 151, 107866.